Progress In Electromagnetics Research M, Vol. 68, 173–180, 2018

Enhanced Characteristic Basis Function Method for Solving the Monostatic Radar Cross Section of Conducting Targets

Jinyu Zhu, Yufa Sun*, and Hongyu Fang

Abstract—In this paper, an enhanced characteristic basis function method (ECBFM) is proposed to calculate the monostatic radar cross section (RCS) of electrical large targets efficiently. The enhanced characteristic basis functions (ECBFs) are defined by combining improved primary-characteristic basis functions (IP-CBFs) with the first level improved secondary-characteristic basis functions (IS-CBFs) for each block. IS-CBFs are obtained by substituting IP-CBFs for PCBFs in Foldy-Lax multiple scattering equation in which mutual coupling effects among all blocks can be included systematically. As a result, a small number of incident plane waves (PWs) is sufficient when dealing with large scale targets. The numerical results demonstrate that the computational efficiency in this paper is much higher than that of the improved primary-characteristic basis function method (IP-CBFM) without losing any accuracy.

1. INTRODUCTION

The method of moments (MoM) [1] is accurate in the analysis of arbitrary three-dimensional electromagnetic scattering. However, with the increase of the size of the targets under analysis, the computational time and memory requirements of the conventional MoM are very expensive. Some fast algorithms such as multilevel fast multipole algorithm (MLFMA) [2], adaptive integral method (AIM) [3] and adaptive cross approximation (ACA) algorithm [4] are proposed to relieve this problem. However, these iterative methods suffer from convergence problems of ill-conditional matrices for electrical large targets. Moreover, when multiple incident plane waves (PWs) scattering problems are considered, the iterative procedure must be repeated for each PW.

The characteristic basis function method (CBFM) [5] effectively reduces the dimension of impedance matrix by dividing the target into several blocks, and high-level basis functions are generated to represent the electromagnetic characteristics of these blocks. These basis functions are referred to as the characteristic basis functions (CBFs), and the CBFs lead to a reduced matrix. Since the method only requires the solution of small size matrix equations, the LU decomposition method [6] can be applied to solve the reduced matrix directly instead of the conventional iterative solving method. In [7], the excitation independent CBFM is proposed by obtaining a set of completely orthogonal primary CBFs (PCBFs), and the set of completely orthogonal PCBFs is used to construct the reduced matrix. This method is widely applied in many aspects, especially for monostatic RCS. Based on the excitation independent CBFM, improved primary-characteristic basis function method (IP-CBFM) [8] is proposed to reduce the number of PWs by combining secondary CBFs (SCBFs) and PCBFs to generate improved primary CBFs (IP-CBFs) of each block. However, IP-CBFM still needs more PWs when dealing with large scale targets, which lead to increasing the time of CBFs generation and reduced matrix filling.

In this paper, an enhanced characteristic basis function method (ECBFM) is proposed to improve the efficiency of numerical calculation for the monostatic radar cross section (RCS). In ECBFM,

Received 27 February 2018, Accepted 25 April 2018, Scheduled 21 May 2018
* Corresponding author: Yufa Sun (yfsun_ahu@sina.com).
The authors are with the Key Lab of Intelligent Computing & Signal Processing, Ministry of Education, Anhui University, Hefei 230601, China.

enhanced characteristic basis functions (ECBFs) consist of IP-CBFs and the first level improved secondary CBFs (IS-CBFs), where IS-CBFs are constructed by solving Foldy-Lax multiple scattering equation [9, 10] in which mutual coupling effects among all blocks can be included systematically. As both IP-CBFs and IS-CBFs are considered, a set of more complete CBFs can be obtained. As a result, a small number of PWs is sufficient when using this set of more complete CBFs. In addition, adaptive cross approximation-singular value decomposition (ACA-SVD) [11] is applied to compress these PWs to reduce the time generation of CBFs in this paper. Numerical results show that ECBFM is more efficient than IP-CBFM and without losing any accuracy.

2. FORMULATION

2.1. The IP-CBFM

The target is divided into M blocks, and the CBFs are composed of PCBFs and SCBFs in IP-CBFM. PCBF is the self-interaction component inside a block. SCBF indicates the mutual interaction component between block i and j ($i = 1, 2, \ldots, M$, $j = 1, 2, \ldots, M$). Let N_θ and N_φ indicate the number of PWs in θ and φ, respectively. Considering two kinds of polarization, the total number of PWs is $N_p = 2N_\theta N_\varphi$, which are arranged in a matrix $\mathbf{E}_{ii}^{N_p}$. PCBF $\mathbf{J}_{ii}^{P}$ for each block can be defined as follows:

$$\mathbf{Z}_{ii}^{e}\mathbf{J}_{ii}^{P} = \mathbf{E}_{ii}^{N_p} \tag{1}$$

where $\mathbf{Z}_{ii}^{e}$ is an $N_i^e \times N_i^e$ extended self-impedance matrix, and $\mathbf{E}_{ii}^{N_p}$ is an $N_i^e \times N_p$ matrix. SCBF $\mathbf{J}_{ij}^{P} (i \neq j)$ for each block can be expressed as

$$\mathbf{Z}_{ii}^{e}\mathbf{J}_{ij}^{P} = -\mathbf{Z}_{ij}^{e'}\mathbf{J}_{jj}^{P'} \ (i \neq j) \tag{2}$$

where $\mathbf{Z}_{ij}^{e'}$ is an $N_i^e \times (N_j - N_{ij}^{overlaping})$ impedance matrix of mutual interaction between block i and j, and $N_{ij}^{overlaping}$ is the portion of the overlap between the extended block i and original block j. According to Eqs. (1) and (2), IP-CBF $\mathbf{J}_{ii}^{IP}$ can be obtained as

$$\mathbf{Z}_{ii}^{e}\mathbf{J}_{ii}^{P} + \sum_{\substack{j=1 \\ j\neq i}}^{M} \mathbf{Z}_{ii}^{e}\mathbf{J}_{ij}^{P} = \mathbf{Z}_{ii}^{e}\sum_{j=1}^{M} \mathbf{J}_{ij}^{P} = \mathbf{Z}_{ii}^{e}\mathbf{J}_{ii}^{IP} = \mathbf{E}_{ii}^{N_p} - \sum_{\substack{j=1 \\ j\neq i}}^{M} \mathbf{Z}_{ij}^{e'}\mathbf{J}_{jj}^{P'} \tag{3}$$

where $\mathbf{J}_{ii}^{IP}$ indicates roughly the correct current distribution of block i, and therefore, the number of PWs can be reduced. It is assumed that all of the blocks contain the same number K of IP-CBFs after ACA-SVD. Then, the dimension of reduced matrix is KM. In addition to the generation of IP-CBFs, this method is the same as CBFM in [7].

2.2. The Formulation of the ECBFM

When dealing with large scale targets, the number of incident PWs required to obtained valid results in IP-CBFM is still large. To solve this problem, IS-CBFs are added to construct ECBFs in IP-CBFM. According to the Foldy-Lax multiple scattering equation, the traditional first level SCBFs $\mathbf{J}_{ii}^{S}$ can be calculated by replacing incident field with scattered field due to the PCBFs on the all blocks except from itself.

$$\mathbf{Z}_{ii}^{e}\mathbf{J}_{ii}^{S} = -\sum_{j=1(j\neq i)}^{M} \mathbf{Z}_{ij}\mathbf{J}_{jj}^{P} \tag{4}$$

IS-CBF is the improvement of the traditional SCBF which is calculated by replacing PCBFs with IP-CBFs in the Foldy-Lax multiple scattering equation. By solving Eq. (5), the first level IS-CBFs $\mathbf{J}_{ii}^{IS}$ can be obtained as

$$\mathbf{Z}_{ii}^{e}\mathbf{J}_{ii}^{IS} = -\sum_{j=1(j\neq i)}^{M} \mathbf{Z}_{ij}\mathbf{J}_{jj}^{IP} \tag{5}$$

where $\mathbf{J}_{ii}^{IP}$ and $\mathbf{J}_{ii}^{IS}$ are the last retained CBFs, which are called as ECBFs $\mathbf{J}_{ii}^{E}$. As both IP-CBFs and IS-CBFs are considered, ECBFs are a set of more complete CBFs which can indicate the correct current distribution more accurately, and therefore, the number of PWs can be further reduced.

Let H_θ and H_φ indicate the numbers of PWs in θ and φ, respectively. The total number of PWs is H_p= $2H_\theta H_\varphi (H_p \ll N_p)$, which are arranged in a matrix $\mathbf{E}_{ii}^{H_p}$ $(i = 1, 2, \ldots, M)$. Moreover, incidents PWs with redundant information are used to calculate CBFs in IP-CBFM, which usually leads to increasing the solving time of CBFs. To mitigate this problem, ACA-SVD is applied to remove the redundancy of PWs as follows in this paper.

First, the ACA of $\mathbf{E}_{ii}^{H_p}$ is expressed as

$$\mathbf{E}_{ii}^{H_p} \simeq \mathbf{E}_U \mathbf{E}_V^T \tag{6}$$

Next, the QR decompositions [12, 13] of $\mathbf{E}_U$ and $\mathbf{E}_V$ are expressed as

$$\mathbf{E}_U = \mathbf{Q}_{i1}\mathbf{R}_1 \tag{7}$$

$$\mathbf{E}_V = \mathbf{Q}_{i2}\mathbf{R}_2 \tag{8}$$

Then, $\mathbf{R}_1\mathbf{R}_2^T$ is recompressed by a truncated SVD

$$\mathbf{R}_1\mathbf{R}_2^T \simeq \mathbf{U}_i\mathbf{S}_i\mathbf{V}_i^T \tag{9}$$

Substituting Eqs. (7)–(9) into Eq. (6)

$$\mathbf{E}_{ii}^{H_p} \simeq \mathbf{Q}_{i1}\mathbf{U}_i\mathbf{S}_i(\mathbf{Q}_{i2}\mathbf{V}_i)^T \tag{10}$$

where the product of $\mathbf{Q}_{i1}\mathbf{U}_i$ is the last retained excitations after a truncated ACA-SVD. Finally, PCBFs $\mathbf{J}_{ii}^{P}$ on the block i can be obtained as

$$\mathbf{Z}_{ii}^{e}\mathbf{J}_{ii}^{P} \simeq \mathbf{Q}_{i1}\mathbf{U}_i \tag{11}$$

Substituting Eq. (11) into Eq. (3), the IP-CBFs $\mathbf{J}_{ii}^{IP}$ can be obtained as

$$\mathbf{Z}_{ii}^{e}\mathbf{J}_{ii}^{IP} = \mathbf{Q}_{i1}\mathbf{U}_i - \sum_{\substack{j=1 \\ j\neq i}}^{M} \mathbf{Z}_{ij}^{e'}\mathbf{J}_{jj}^{P'} \tag{12}$$

Then, substituting $\mathbf{J}_{ii}^{IP}$ into Eq. (5), $\mathbf{J}_{ii}^{IS}$ can be obtained. For the sake of simplicity, it is assumed that all of the blocks contain the same number K_E of IP-CBFs after ACA-SVD. Thus, the number of $\mathbf{J}_{ii}^{E}$ is $2K_E$, and the dimension of reduced matrix is $2K_EM (2K_EM \ll KM)$. Moreover, in order to reduce the time of CBFs generation, ACA-SVD is also used to compress incident PWs in IP-CBFM. However, although compression of incident PWs is used in the two methods, ECBFM is more efficient than IP-CBFM in CBFs generation, since it requires only a small number of incident PWs.

3. NUMERICAL RESULTS

In this section, several numerical examples were studied to demonstrate the accuracy and efficiency of the proposed method. The ACA and SVD threshold are chosen to be 10-3. All the results are computed on the Intel® Core™ i7-3820 3.60 GHz, 64 GB RAM PC. The compiler uses Code Blocks. The relative error is defined as follows:

$$Err(\%) = 100 \times \sqrt{\sum_n |RCS^{\chi} - RCS^{FEKO}|^2} \Big/ \sqrt{\sum_n |RCS^{FEKO}|^2} \tag{13}$$

where RCS^{χ} are the results of IP-CBFM and ECBFM, and RCS^{FEKO} are the simulation results of the software FEKO.

First, the monostatic RCS of a PEC cylinder with 4 m length and 0.25 m radius at a frequency of 400 MHz is calculated. The geometry is divided into 2112 triangular patches, and the number of unknowns is 5696, which is divided into 16 blocks, and each block is extended by 0.15λ in all directions. The incidence angle is set to $\theta = 0°$–$180°$, $\varphi = 0°$. Incident PWs of PEC Cylinder are shown in Figure 1,

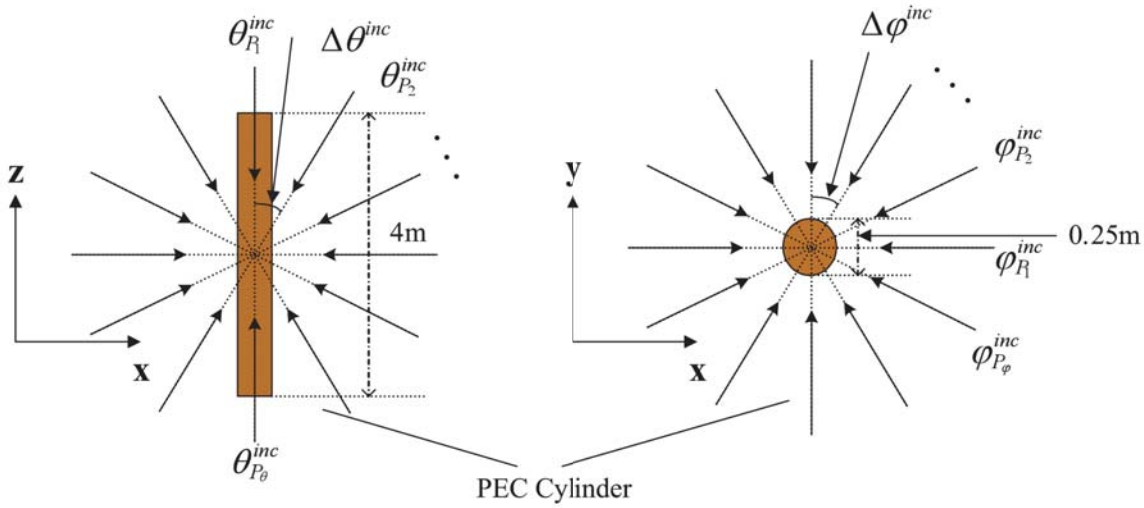

Figure 1. Incident PWs of PEC Cylinder.

Table 1. The analysis conditions of two methods.

Method	(P_θ, P_φ)	$(\Delta\theta^{inc}, \Delta\varphi^{inc})$	Number of PWS
IP-CBFM-1	(9, 4)	(22.5°, 90°)	72
IP-CBFM-2	(9, 8)	(22.5°, 45°)	144
ECBFM	(9, 2)	(22.5°, 180°)	36

and the analysis conditions of two methods are shown in Table 1. For convenience, P_θ, P_φ are used to denote the numbers of incident PWs in θ and φ, respectively. $\Delta\theta^{inc}, \Delta\varphi^{inc}$ indicate angle intervals of incident PWs. IP-CBFM-1 and IP-CBFM-2 represent the IP-CBFM with different numbers of incident PWs.

The results of monostatic RCS in HH and VV polarizations are calculated by IP-CBFM, and the proposed ECBFM and FEKO are shown in Figure 2 and Figure 3.

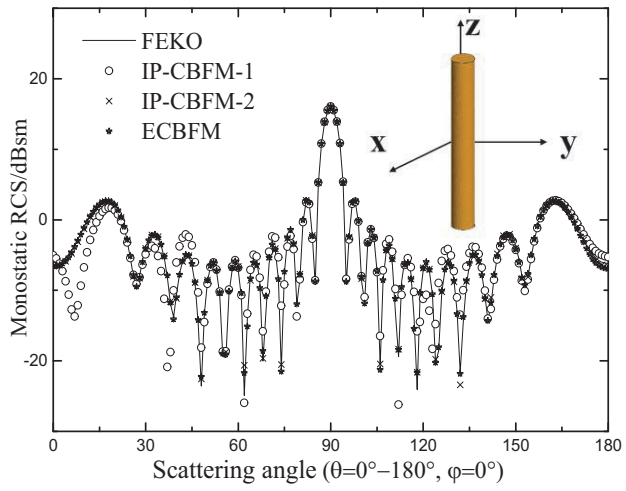

Figure 2. HH polarization monostatic RCS of Cylinder.

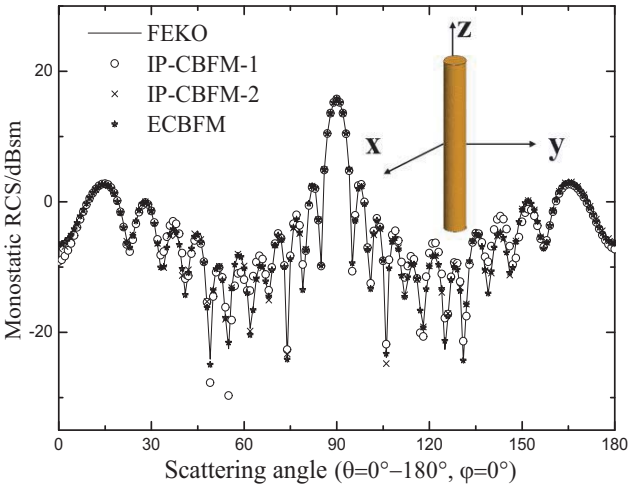

Figure 3. VV polarization monostatic RCS of Cylinder.

It can be seen in Figure 2, Figure 3 and Table 1 that IP-CBFM-1 with 72 PWs cannot obtain valid results. The results of IP-CBFM-2 and ECBFM are in good agreement with those of FEKO. The calculation time and relative error of the two methods are presented in Table 2.

Table 2. The calculation time and relative error of two methods.

Method	CBFs generation time (s)	Reduced matrix filling time (s)	Total time (s)	Dimension of reduced matrix	Relative error in HH polarization (%)	Relative error in VV polarization (%)
IP-CBFM-1	-	-	-	-	33.61	18.26
IP-CBFM-2	13.05	107.99	149.16	1215	5.96	4.21
ECBFM	6.78	59.12	88.68	886	5.17	2.95

It can be found easily from Table 2 that the proposed ECBFM outperforms the IP-CBFM in computation time and accuracy. The dimension of reduced matrix is reduced by 27.1%, and computational efficiency is increased by 40.5%.

Next, the monostatic RCS of 25 discrete PEC cubes with the length 1.0 m and the spacing between two cubes 1.0 m at the frequency of 250 MHz are computed and compared. The target is divided into 19000 triangular patches, and the number of unknowns is 28500. The target is just divided into 25 blocks. The incidence angle is set to $\theta = 0°$–$180°$, $\varphi = 0°$. Table 3 shows the analysis conditions of two methods. The results of monostatic RCS in HH and VV polarizations calculated by IP-CBFM, ECBFM and FEKO are shown in Figure 4 and Figure 5. The calculation time and relative error of two methods are presented in Table 4.

Table 3. The analysis conditions of two methods.

Method	(P_θ, P_φ)	$(\Delta\theta^{inc}, \Delta\varphi^{inc})$	Number of PWS
IP-CBFM-1	(20, 6)	(9.5°, 60°)	240
IP-CBFM-2	(16, 9)	(12°, 40°)	288
ECBFM	(9, 2)	(22.5°, 180°)	36

Table 4. The calculation time and relative error of two methods.

Method	CBFs generation time (s)	Reduced matrix filling time (s)	Total time (s)	Dimension of reduced matrix	Relative error in HH polarization (%)	Relative error in VV polarization (%)
IP-CBFM-1	-	-	-	-	26.55	40.75
IP-CBFM-2	422.27	19594.14	20242.21	2809	7.07	11.93
ECBFM	209.83	6439.19	6815.69	1606	2.34	2.89

It can be seen in Figure 4, Figure 5 and Table 3 that IP-CBFM-1 with 240 PWs cannot obtain valid results, and even the results of IP-CBFM-2 cannot be in good agreement with those of FEKO, especially for VV polarization. However, the results of ECBFM are in good agreement with those of FEKO.

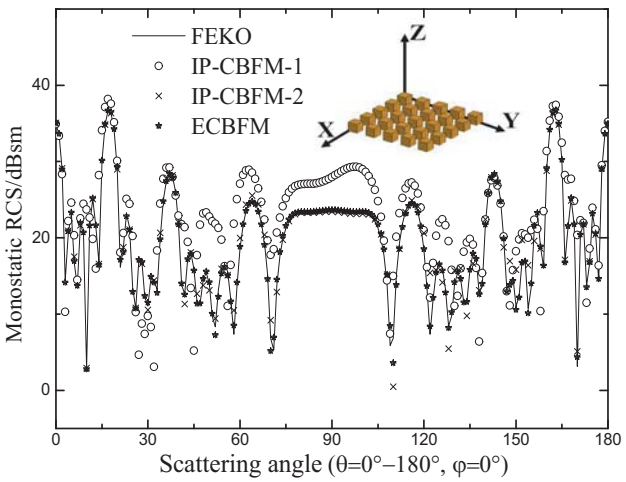

Figure 4. HH polarization monostatic RCS of Discrete Cubes.

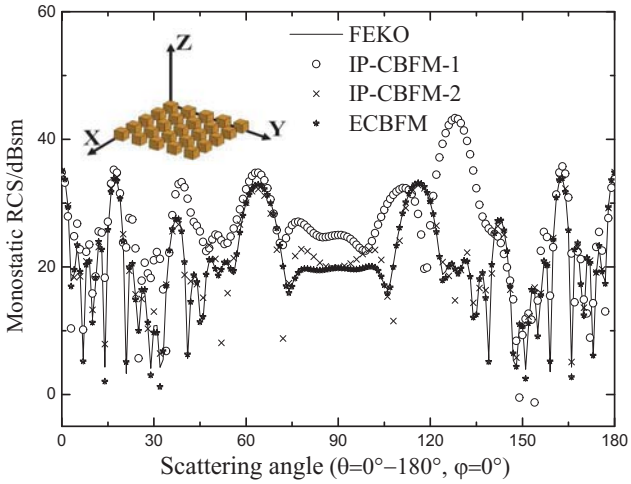

Figure 5. VV polarization monostatic RCS of Discrete Cubes.

It can be easily seen from Table 4 that the proposed ECBFM performs better than IP-CBFM in computation time and accuracy. Moreover, the dimension of reduced matrix is reduced by 42.8%, and computational efficiency is increased by 66.3%.

To further prove the accuracy and efficiency of the proposed method, the monostatic RCS of a PEC almond with 252.3744 mm at 6 GHz has been calculated. The target is divided into 20 blocks, and each block is extended by 0.2λ in all directions. The target is divided into 6236 triangular patches, and the total number of unknowns is 23161. The incidence angle is set to $\theta = 90°$, $\varphi = 0°$–$180°$. The analysis conditions of two methods are shown in the Table 5.

Table 5. The analysis conditions of two methods.

Method	(P_θ, P_φ)	$(\Delta\theta^{inc}, \Delta\varphi^{inc})$	Number of PWS
IP-CBFM-1	(8, 6)	(25.5°, 60°)	96
IP-CBFM-2	(9, 7)	(22.5°, 51.5°)	126
ECBFM	(6, 4)	(36°, 90°)	48

The results of monostatic RCS in HH and VV polarizations calculated by IP-CBFM, proposed ECBFM and FEKO are shown in Figure 6 and Figure 7. The calculation time and relative error of two methods are presented in Table 6.

Table 6. The calculation time and relative error of two methods.

Method	CBFs generation time (s)	Reduced matrix filling time (s)	Total time (s)	Dimension of reduced matrix	Relative error in HH polarization (%)	Relative error in VV polarization (%)
IP-CBFM-1	150.98	853.89	1192.42	1379	4.92	9.27
IP-CBFM-2	191.65	1143.89	1540.11	1654	1.50	1.61
ECBFM	126.15	945.95	1259.83	1422	0.98	1.55

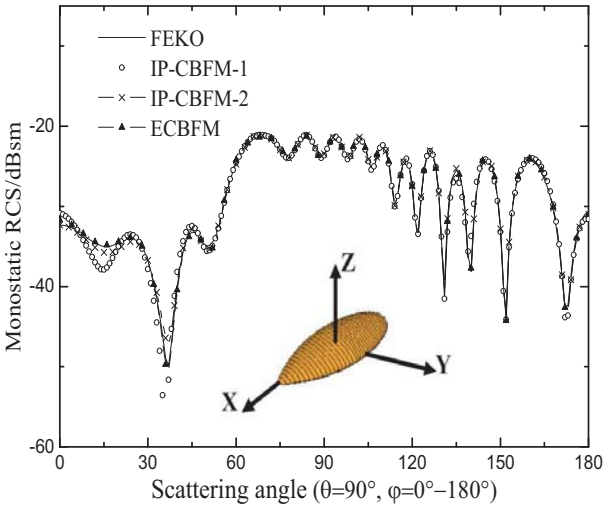

Figure 6. HH polarization monostatic RCS of Almond.

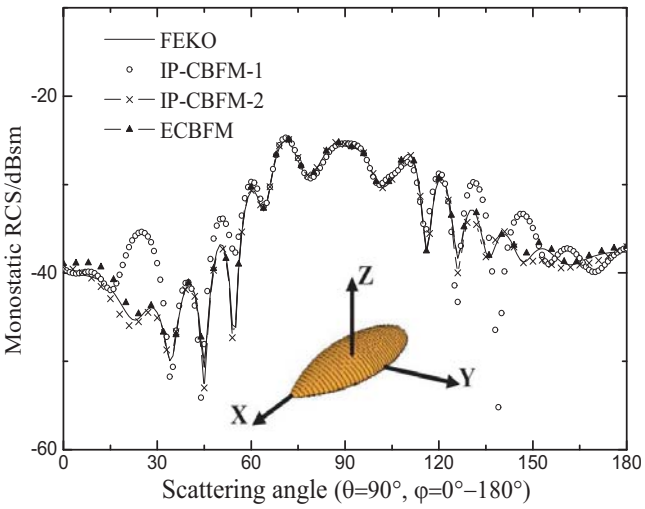

Figure 7. VV polarization monostatic RCS of Almond.

It can be seen in Figure 6, Figure 7 and Table 5 that IP-CBFM-1 with 96 PWs cannot obtain valid results, especially for VV polarization. However, the results of IP-CBFM-2 and ECBFM are in good agreement with those of FEKO. It can be easily seen from Table 6 that the proposed ECBFM performs better than IP-CBFM in computation time and accuracy, especially for HH polarization.

4. CONCLUSION

In this paper, an ECBFM is proposed to solve the multiple incident PWs monostatic RCS of electrical large targets rapidly. ECBFs are defined and consist of IP-CBFs and first level IS-CBFs according to Foldy-Lax multiple scattering equation. The proposed method can reduce the time of CBFs generation and reduced matrix filling significantly only with a small number of the incident PWs compared to IP-CBFM without losing any accuracy. The numerical results demonstrate that the proposed method is accurate and efficient.

ACKNOWLEDGMENT

This work is supported by the National Natural Science Foundation of China under Grant 61172020.

REFERENCES

1. Harrington, R. F., *Field Computation by Moment Methods*, IEEE Press, New York, 1993.
2. Song, J., C. C. Lu, and W. C. Chew, "Multilevel fast multipole algorithm for electromagnetic scattering by large complex objects," *IEEE Trans. Antennas Propag.*, Vol. 45, No. 10, 1488–1493, 1997.
3. Bleszynski, E., M. Bleszynski, and T. Jaroszewicz, "Adaptive integral method for solving large-scale electromagnetic scattering and radiation problems," *Radio Science*, Vol. 31, No. 5, 1225–1251, 1996.
4. Zhao, K., M. N. Vouvakis, and J. F. Lee, "The adaptive cross approximation algorithm for accelerated method of moments computations of EMC problems," *IEEE Transactions on Electromagnetic Compatibility*, Vol. 47, No. 4, 763–773, 2005.
5. Kwon, S. J., K. Du, and R. Mittra, "Characteristic basis function method: A numerically efficient technique for analyzing microwave and RF circuits," *Microwave & Optical Technology Letters*, Vol. 38, No. 6, 444–448, 2003.

6. Pan, P. Q., "A projective simplex algorithm using LU decomposition," *Computers & Mathematics with Applications*, Vol. 39, No. 1, 187–208, 2000.
7. Lucente, E., A. Monorchio, and R. Mittra, "An iteration-free MoM approach based on excitation independent characteristic basis functions for solving large multiscale electromagnetic scattering problems," *IEEE Trans. Antennas Propag.*, Vol. 56, No. 4, 999–1007, 2008.
8. Tanaka, T., Y. Inasawa, Y. Nishioka, and H. Miyashita, "Improved primary-characteristic basis function method for monostatic radar cross section analysis of specific coordinate plane," *IEICE Transactions on Electronics*, Vol. E99, No. 1, 28–35, 2016.
9. Tsang, L., C. E. Mandt, K. H. Ding, and V. F. T. Article, "Monte Carlo simulations of the extinction rate of dense media with randomly distributed dielectric spheres based on solution of Maxwell's equations," *Optics Letters*, Vol. 17, No. 5, 314–316, 1992.
10. Sun, Y. F., C. H. Chan, and R. Mittra, "Characteristic basis function method for solving large problems arising in dense medium scattering," *IEEE Antennas and Propagation Society International Symposium*, Vol. 2, 1068–1071, 2003.
11. Bebendorf, M. and S. Kunis, "Recompression techniques for adaptive cross approximation," *Journal of Integral Equations & Applications*, Vol. 21, No. 2009, 331–357, 2007.
12. Seo, S. M. and J. F. Lee, "A single-level low rank IE-QR algorithm for PEC scattering problems using EFIE formulation," *IEEE Trans. Antennas Propag.*, Vol. 52, No. 8, 2141–2146, 2004.
13. Burkholder, R. J. and J. F. Lee, "Fast dual-MGS block-factorization algorithm for dense MoM matrices," *IEEE Trans. Antennas Propag.*, Vol. 52, No. 7, 1693–1699, 2004.